Mine Water and the Environment (2018) 37:686–695
https://doi.org/10.1007/s10230-018-0514-4

TECHNICAL ARTICLE

Changes in Efficiency and Hydraulic Parameters During the Passive Treatment of Ferriferous Acid Mine Drainage in Biochemical Reactors

Thomas Genty[1] · Bruno Bussière[1] · Mostafa Benzaazoua[1] · Carmen M. Neculita[1] · Gérald J. Zagury[2]

Received: 14 June 2017 / Accepted: 7 January 2018 / Published online: 22 January 2018

Abstract

The objective of this study was to evaluate the effects of different reactive mixtures and hydraulic retention times (HRTs) on hydraulic parameters (hydraulic conductivity, k_{sat}, and porosity) and the efficiency of passive biochemical reactors (PBRs) for treatment of ferriferous acid mine drainage (AMD). Five 10.7 L PBRs were filled with three reactive mixtures, containing either a carbon-rich substrate (60% w/w) or an inert/neutralizing agent (50% w/w). The PBRs were tested over a 450 day period using two qualities of iron-rich AMD (4 and 1 g L^{-1} Fe in AMD1 and AMD2, respectively), and two HRTs, of 5 and 7 days. During the last week of the columns' operation, a tracer test (5 g L^{-1} of NaCl) was also performed, in addition to monthly measurements using the falling head method. Changes in HRT and k_{sat} were evaluated throughout the experiment. The PBRs increased the pH of AMD influents from 3.5 to 6 and efficiently removed Al, Cd, Cr, Ni, Pb, and Zn (> 90%), whereas Fe was only partially and inconsistently treated. No significant differences were observed among the three tested mixtures, regardless of the HRT or the AMD quality. Results from the tracer test and k_{sat} measurements showed no significant decrease in the initial values of the hydraulic parameters with time except for column 3, where a slight decrease was observed. Although sorption could have been important during the start-up of the PBRs, post-testing characterization of the spent reactive mixtures showed that the Fe was mainly retained as oxy-hydroxides and sulfides. Given the PBRs' marginal effectiveness for Fe-rich AMD, pre-treatment removal of the iron is recommended.

Keywords Reactive mixture · Retention time · Hydraulic conductivity · Metal removal mechanisms · Tracer test

Introduction

Various active and passive technologies are available for acid mine drainage (AMD) treatment. Active treatment is generally relied on by operating mines, whereas passive systems are generally used as complementary tools for the reclamation of closed or abandoned mines sites, primarily because they use natural or residual materials and involve lower investments of capital and energy (Neculita et al. 2007; Skousen et al. 2017; USEPA 2014). Limestone or dolomitic drains and passive biochemical reactors (PBRs) have been successfully used to treat moderately contaminated AMD (USEPA 2014). In PBRs, fermentative organisms provide electron donors by decomposing complex organic matter, while sulfate- and metal-reducing microbes use these electron donors to produce products that lead to metal immobilization (Baldwin et al. 2015). Laboratory and field observations show that precipitation of biosulfides is only one removal mechanism, with other mechanisms including sorption and precipitation of metals as hydroxides and carbonates (Lewis 2010; USEPA 2014).

However, passive treatment of ferriferous AMD, i.e. iron-rich (> 500 mg L^{-1} Fe), is still very challenging. To date, a relatively limited number of studies are available on this topic (Ayora et al. 2013; Chang et al. 2000; Genty et al. 2011, 2012a, b, 2016, 2017; Neculita et al. 2008a, b; Rötting et al. 2008; Rakotonimaro et al. 2016, 2017; Zagury et al. 2006). Laboratory and field-scale studies found that

---

Electronic supplementary material The online version of this article (https://doi.org/10.1007/s10230-018-0514-4) contains supplementary material, which is available to authorized users.

✉ Gérald J. Zagury
Gerald.Zagury@polymtl.ca

[1] Research Institute on Mines and Environment (RIME), University of Québec in Abitibi-Témiscamingue (UQAT), Rouyn-Noranda, QC J9X 5E4, Canada

[2] Department of Civil, Geological, and Mining Engineering, Polytechnique Montréal, RIME-Polytechnique Montréal, Montreal, QC H3C 3A7, Canada

multi-step systems, consisting of chemical and biochemical, aerobic and anaerobic units, were more appropriate to limit clogging and extend the lifespan and efficiency of passive treatment systems in the case of highly contaminated AMD (Ayora et al. 2013; Champagne et al. 2005; Rötting et al. 2008). The development of a passive treatment system known as dispersed alkalinity substrate (DAS), which consists of a mixture of a coarse organic material (e.g. wood chips) and a neutralizing agent (e.g. calcite—$CaCO_3$ or magnesia—MgO), showed promising results for the treatment of metals in highly contaminated AMD, including both trivalent (Fe, up to 1.5 g L^{-1}) and bivalent (Zn, up to 0.6 g L^{-1}) species (Ayora et al. 2013; Genty et al. 2016, 2017; Rakotonimaro et al. 2016, 2017; Rötting et al. 2008).

However, AMD at closed and abandoned metal mine sites is sometimes characterized by much higher iron concentrations (up to 141 g L^{-1} Fe, in extreme cases, such as at Iron Mountain, CA, USA), whereas most of the divalent metals are present at lower concentrations (Moncur et al. 2005). The efficiency of passive treatment for iron-rich AMD is severely limited, primarily by changes in the hydraulic parameters of the systems, which lead to decreased porosity and permeability and, finally, to clogging and drastic limitation of gravity flow (Ayora et al. 2013; Bolis et al. 1992; Neculita et al. 2008b; Younger et al. 2002). The main metal removal mechanism during ferriferous AMD treatment in PBRs is precipitation as oxyhydroxides, carbonates, and sulfides; sulfides may represent a minor proportion (up to 15%, for around 500 mg L^{-1} Fe in AMD; Neculita et al. 2008b).

The efficient removal of iron from Fe-rich AMD (500 mg L^{-1} Fe) was reported in column PBRs (filled with fresh and spent oak chips, spent mushroom compost, waste paper sludge, or organic-rich soil) at 20 days of hydraulic retention time (HRT) over 20 weeks, but residual concentrations progressively increased afterwards until the end of testing, at week 35 (Chang et al. 2000). However, no hydraulic parameters were measured in this study (Chang et al. 2000). A reactive mixture consisting of a four-material substrate (manure, wood chips, sawdust, and compost) and inorganic components (sand, sediment, and calcite) was also found to be efficient in the treatment of iron-rich AMD in six 3.5 L column PBRs (with HRTs of 7.3 and 10 days, over a 15-month period; Neculita et al. 2008a). Severe decreases in porosity (from 0.34 to 0.43 to very low values) and k_{sat} (from 2.3×10^{-2} to 2×10^{-5} cm s^{-1}, with an HRT of 7.3 days) were observed at the end of the testing period, after 38 weeks of operation (7.3×10^{-9} cm s^{-1} at 10 days of HRT; Neculita et al. 2008b). The suspected cause for the drastic reduction in the k_{sat} was the build-up of iron oxyhydroxides in the top layer and/or the accumulation of metal biosulfides in the bottom layer of the reactors. The decrease in k_{sat} in a one-dimensional flow column was previously stressed by Seki et al. (2006). The presence of residual iron, either dissolved or as nanoparticles, could also cause acute toxicity in treated effluent (Butler et al. 2011; Neculita et al. 2008c; Seo et al. 2010).

The present study is a follow-up of a previous investigation (Genty et al. 2017), where the role of sorption in iron removal was assessed through batch testing; this study allowed for the selection of the most promising reactive mixtures for the treatment of iron-rich AMD in column PBRs. The objective of the present study was to evaluate the effects of different reactive mixtures and HRTs on hydraulic parameters (k_{sat} and porosity) and the efficiency of PBRs in the treatment of ferriferous AMD.

Materials and Methods

Column Set-up and Operation

Three reactive mixtures (Table 1) were previously selected through batch testing (Genty et al. 2017). Two qualities of synthetic AMD (AMD1 = 4 g L^{-1} Fe, AMD2 = 1 g L^{-1} Fe; Table 2) and two HRTs (5 and 7 days) were tested in five 10.7 L Plexiglas column PBRs (14 × 70 cm), over a 450 day period.

The PBR columns contained mixtures #1, #2, and #3, or mixtures #2D and #3D, which were duplicates of columns #2 and #3, respectively. As indicated in Table 1, the tests were performed with either powdered calcium carbonate (ACS chemical) or limestone (≈ 96% calcite, with minor amounts of quartz, and other crystal forms of calcium carbonate) as neutralizing material. During the first 173 days and after 229 days, the HRT was set at 5 days

Table 1 Composition (% dry mass) of the reactive mixtures used in column PBRs

Mixture	#1	#2	#3
Cellulosic wastes			
Maple wood chips	10	5	6
Maple sawdust	20	10	11
Organic wastes			
Chicken manure	10	5	8
Leaf compost	20	10	12
Inoculum			
Sediment	15	8	8
Inert structural agent			
Sand	20	10	50
Nutrient (nitrogen)			
Urea	3	2	3
Neutralizing agent			
Calcium carbonate (99% purity)	2		2
Limestone rock (96% purity)		50	

Table 2 Characteristics of the two qualities of synthetic AMD (in mg L^{-1}, except for pH)

Parameters	Concentration (mg L^{-1})	Salt used
Al	7	$Al_2(SO_4)_3 \cdot 18H_2O$
Cd	0.5	$CdSO_4 \cdot 8H_2O$
Cr	1	$CrK(SO_4)_2 \cdot 12H_2O$
Fe	4000/1000	$FeSO_4 \cdot 7H2O$
Mg	10	$MgSO_4 \cdot 7H_2O$
Mn	10	$MnSO_4 \cdot H_2O$
Ni	2	$NiSO_4 \cdot 6H_2O$
Pb	0.5	$Pb(NO_3)_2$
SO_4^{2-}	9000	$Na_2SO_4 \cdot 10H_2O$
Zn	0.5	$ZnSO_4 \cdot 7H_2O$
pH	3.5	

(0.6 mL min^{-1}); between 173 and 229 days, the HRT was set at 7 days (0.4 mL min^{-1}). Testing started with 4 g L^{-1} Fe (AMD1) and, after 55 days, was decreased to 1 g L^{-1} Fe (AMD2); after 229 days, the AMD1 influent was reinstated. Columns #2D and #3D were fed with AMD1 using an HRT of 5 days throughout the experiment.

The columns were fed by peristaltic pumps, in a vertical downward flow, with ferriferous AMD to allow for the progressive development of anoxic conditions. A perforated plastic plate covered with a geotextile was placed at the bottom of the columns to ensure the even distribution of the feed. After their set-up, all PBRs were saturated with Postgate B medium, prepared in distilled water, with the following composition: 3.5 g L^{-1} sodium lactate (or 4.7 mL of 56.8% lactate liquid); 2.0 g L^{-1} $MgSO_4 \cdot 7H_2O$; 1.0 g L^{-1} NH_4Cl; 1.27 g L^{-1} $CaSO_4 \cdot 2H_2O$; 1.0 g L^{-1} yeast extract; 0.5 g L^{-1} KH_2PO_4; 0.5 g L^{-1} $FeSO_4 \cdot 7H_2O$; 0.1 g L^{-1} thioglycolic acid, and 0.1 g L^{-1} ascorbic acid (Postgate 1984). Then, the PBRs were incubated at ambient temperature for four weeks (i.e. rough acclimation period for anaerobic bacteria) prior to the beginning of the experiment. During this period, weekly samples were collected from the columns' effluent and the Eh was measured. AMD input began when the Eh was below −150 mV (Neculita et al. 2008a). The efficiency of the PBRs was evaluated based on parameters measured in influent and effluent samples collected during the 450 days of testing (284 days for column #1). These parameters included: pH, Eh, acidity, alkalinity, and sulfate and metal concentrations. Counts of sulfate-reducing bacteria (SRB) were also performed for all columns using the most-probable number (MPN) technique (ASTM 2009).

Evaluation of Hydraulic Parameters

The initial porosity of the reactive mixtures was estimated by the volume of Postgate B medium needed to saturate the columns, and ranged from 0.40 to 0.46. Changes in k_{sat} and HRT were evaluated over the duration of the column tests. Significant decreases in k_{sat} are generally interpreted as an indication of clogging (Bolis et al. 1992; Neculita et al. 2008a). The k_{sat} was evaluated monthly using the falling head method (ASTM 1995). A tracer test (5 g L^{-1} of NaCl mixed into the AMD feed) was also performed during the last week of operation in column #2 in order to estimate the actual HRT. Because the flow rate was too small to use a pulse tracer test, injection reproduced a one-step tracer test, which consisted of increasing and maintaining the chloride concentrations in the AMD close to 0–5 g L^{-1} over an 11 day period (Fogler 2006). Residual chloride concentrations in the column #2 effluent were used to draw the breakthrough curve. Chloride concentrations were determined using a Metrohm 881 compact IC (pro Ions chromatograph, with chemical and CO_2 suppressor, column Metrosep A supp 5-150/4.0, eluent: 3.2 mmol Na_2CO_3 and 1 mmol $NaHCO_3$, flow rate: 0.7 mL min^{-1}).

Analytical Methods for Evaluating Influent and Effluent Quality

The pH and Eh were measured immediately after sampling (Benchtop pH/ISE meter, Orion model 920). The alkalinity and acidity were determined by titrating non-filtered samples with 0.02N H_2SO_4 to a pH of 4.5, and with 0.1 N NaOH to a pH 8.3, respectively (APHA 2005). Filtered (0.45 µm) and acidified (2% nitric acid) samples were used to determine metal (Al, Cd, Cr, Fe, Pb, Ni, and Zn) concentrations through inductively coupled plasma atomic emission spectrometry (ICP-AES, Perkin Elmer OPTIMA 3100 RL). Sulfate concentrations were determined using a nephelometric method (AFNOR 1986) and an Ultraspec 2100 pro spectrometer (relative precision of $\pm 0.5\%$).

Samples of spent reactive mixtures from the middle sections of each PBR were collected at the end of the testing period, and rapidly frozen to prevent sulfide oxidation. No visible difference in color between the top and bottom layers was found during dismantlement. Total sulfur was determined for samples from the top, middle, and bottom layers using a carbon/sulfur analyzer (ELTRA CS 2000); these analyses showed no significant differences. Physicochemical analyses were carried out on water extracts (1:10 solid: liquid ratio) of solid samples using standard methods (APHA 2005). These analyses included: total organic carbon (TOC), total Kjeldahl nitrogen (TKN), and dissolved organic carbon (DOC). Prior to analysis of total metal (Al, Cd, Cr, Fe, Ni, and Zn) concentrations, solid samples were digested in a mixture of strong acids (10 mL HNO_3, 1 mL Br_2, 10 mL HCl, and 1–2 mL HF). To assess the stability of metal precipitates and their potential mobility in spent reactive mixtures, leaching techniques (i.e. a sequential extraction procedure—SEP) and mineralogical characterisations were used. The SEP (Zagury et al. 1997) previously allowed for the collection of useful information on metal removal mechanisms in spent reactive mixtures collected from PBRs (Neculita et al. 2008a). The SEP allowed for separation of: (a) fraction 1: soluble and exchangeable metals; (b) fraction 2: carbonate-bound metals; (c) fraction 3: reducible or metals bound to Fe–Mn oxides; (d) fraction 4: oxidizable or metals bound to organic matter; and (e) fraction 5: residual metals. More details on the procedure are provided elsewhere (Neculita et al. 2008a; Zagury et al. 1997).

Mineralogical characterisation was performed using scanning electron microscopy (SEM) coupled with X-ray microanalysis (Hitachi 3500-N) and energy dispersive spectrometry (EDS) of an X-ray probe (20 keV, 140 A, 25 kPa, and a working distance of 15 mm). Liquid–solid chemical equilibria were estimated by geochemical equilibrium modeling using Visual MINTEQ (ver. 2.53).

Results

In order to follow the effects of changes made to the columns during their operation (Table 3), and for the purposes of discussion, the results of this study (Fig. 1) were divided into five time periods. The geochemical data from treated effluents in the duplicate columns, over a 64 day period, were interpreted using paired difference tests (Mendelhall and Beaver 1994). Results demonstrated that pH, Eh, and alkalinity, acidity, iron, and sulfate concentrations can be considered as originating from the same population (confidence interval of 95%), i.e. from identical tests. Additional information is provided elsewhere (Genty et al. 2011). Maximum iron uptake capacity (q_{max}) of the three reactive mixtures was also evaluated in a previous study and showed values of 8.1, 3.2, and 3.7 mg g^{-1} for columns #1, #2, and #3, respectively (Genty et al. 2017).

Table 3 Physicochemical parameters and geochemical data of feed and treated effluent in column PBRs

	pH	Eh	Alkalinity	Iron	Sulfates	Iron removal %			Sulfate removal %		
		(mV)	(mg L^{-1} $CaCO_3$)	(g L^{-1})	(g L^{-1})	Av.	Min	Max	Av.	Min	Max
Period 1 (0–55 days): 5 days of HRT, 4 g L^{-1} Fe											
AMD1	2.8	555	0	3.71	9.93	–	–	–	–	–	–
#1	6.7	31	3820	2.23	8.80	36	0	99	21	9	41
#2	6.5	7	2610	1.72	8.69	49	6	98	24	1	42
#3	6.2	30	1740	2.62	10.0	26	2	75	14	1	31
Period 2 (56–173 days): 5 days of HRT, 1 g L^{-1} Fe											
AMD2	3.2	498	0	1.21	8.85	–	–	–	–	–	–
#1	6.2	11	521	0.96	8.42	33	5	66	8	0	21
#2	6.2	29	327	0.98	9.30	29	8	45	9	4	24
#3	6.2	16	373	0.97	8.13	27	1	47	11	4	22
Period 3(174–229 days): 7 days of HRT, 1 g L^{-1} Fe											
AMD2	3.2	498	0	1.21	8.85	–	–	–	–	–	–
#1	6.2	27	496	0.63	8.77	47	23	66	11	10	11
#2	6.2	25	571	0.62	8.99	50	38	45	7	6	9
#3	6.3	16	485	0.73	8.87	37	16	47	10	8	11
Period 4 (230–291 days): 7 days of HRT, 4 g L^{-1} Fe											
AMD2	2.8	555	0	3.71	9.93	–	–	–	–	–	–
#1	6.1	52	525	1.79	9.80	32	10	55	8	4	12
#2	6.1	46	430	2.43	9.82	22	5	45	4	2	6
#3	6.2	45	375	2.16	9.96	28	9	60	5	1	7
Period 5 (292–450 days): 5 days of HRT, 4 g L^{-1} Fe											
AMD1	2.8	555	0	3.71	9.93	–	–	–	–	–	–
#1	6.1	23	343	3.19	9.75	No available data					
#2	6.1	33	241	3.36	9.63	18	0	50	8	4	16
#3	6.1	57	201	3.39	9.47	14	2	36	7	0	14

The data (#1, #2, and #3) are for the end of each operating period (1–5)

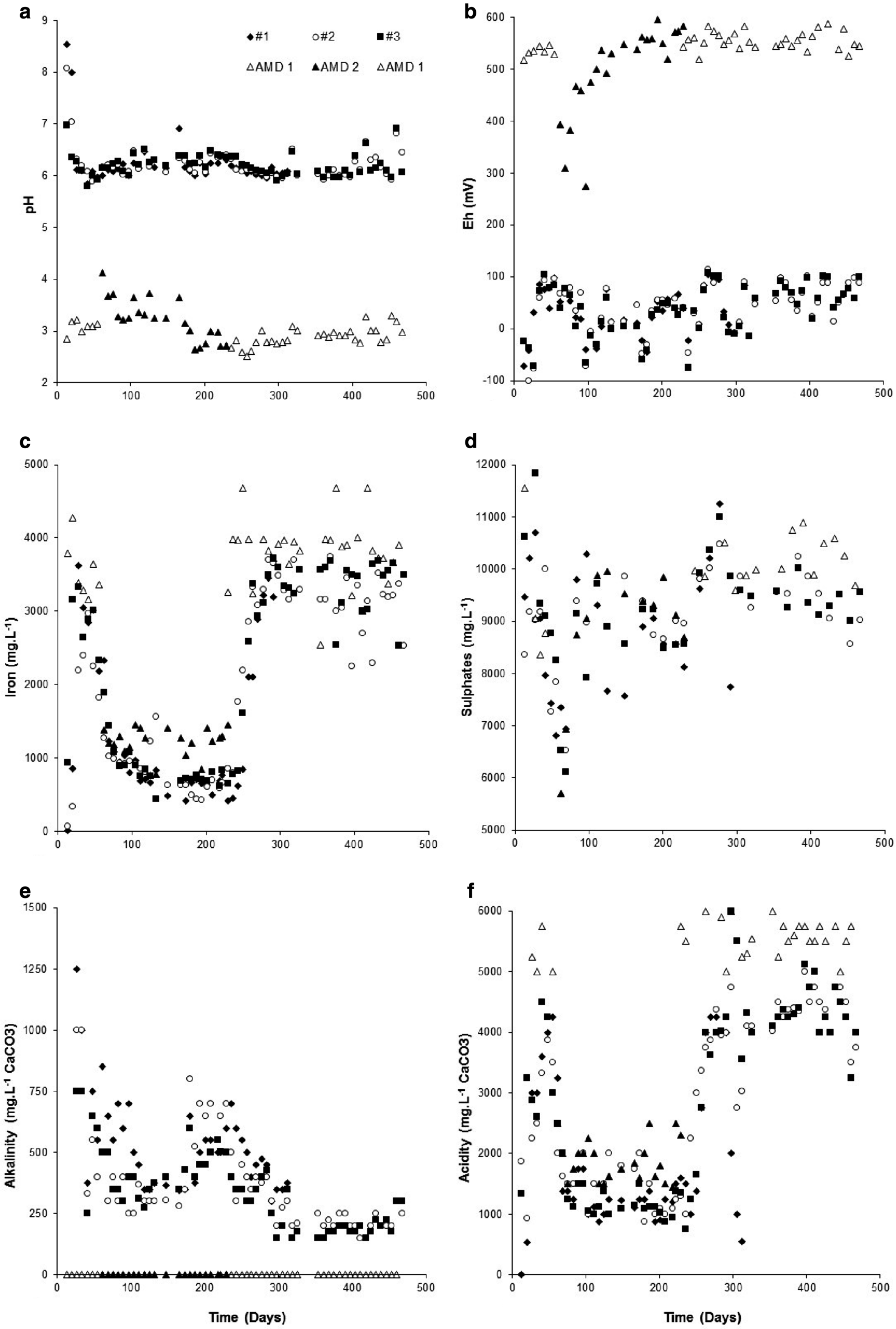

Fig. 1 Evolution of **a** pH, **b** Eh, **c** iron concentration, **d** sulfate concentration, **e** alkalinity, and **f** acidity in column PBRs

Period 1 (Days 0–55): 5 Day HRT and 4 g L^{-1} Fe

During period 1, the pH in columns #1, #2, and #3 decreased rapidly from between 7 and 8.6 to between 6.2 and 6.7 (Fig. 1a), while the Eh ranged between − 100 and 100 mV (Fig. 1b). Effluent iron concentrations (Fig. 1c) were low after the first week of operation for mixtures #1 and #2 (13 and 64 mg L^{-1}, respectively), but high for mixture #3 (939 mg L^{-1}). Concentrations then increased progressively to approximately 2.7 g L^{-1} on day 55. After starting up the PBRs, Fe removal efficiency was between 75 and 99%, depending on the column, but rapidly decreased to close to 0, before increasing again and stabilizing at 30–45%, on day 55 (Table 3). Sulfate concentrations ranged from 8.4 to 12.6 g L^{-1} in the influent (Fig. 1d), and from 6.8 to 10.7 g L^{-1} in the effluent from column #1, 7.3–10 g L^{-1} from column #2, and 8.25 to 12.2 g L^{-1} from column #3. Alkalinity decreased from 10.8 g L^{-1} $CaCO_3$ and stabilized between 400 and 700 mg L^{-1} $CaCO_3$ (Fig. 1e), whereas acidity increased in all columns (Fig. 1f) from 1.1 g L^{-1} $CaCO_3$ to up to 4 g L^{-1} $CaCO_3$ on day 55.

Period 2 (Days 55–173): 5 Day HRT and 1 g L^{-1} Fe

During period 2, the pH in all columns remained stable at around 6.2, while Eh varied slightly (11–29 mV). Iron concentrations in the effluent decreased and stabilized at similar values (955 to 980 mg L^{-1}), which correspond to an iron removal efficiency of 27–33%. Sulfate concentrations in the effluent were lower than in the AMD (8–11% removal), with minimum values in column #1, at 7.35 g L^{-1}. Acidity and alkalinity stabilized at 1–2 g L^{-1} as $CaCO_3$ and at 327 to 521 mg L^{-1} as $CaCO_3$, respectively, with the highest alkalinity generation in column #1.

Period 3 (Days 174–229): 7 Day HRT and 1 g L^{-1} Fe

During period 3, the pH stayed close to 6.2, while Eh oscillated between 16 and 27 mV (Table 3). Iron concentrations progressively decreased (615–732 mg L^{-1}), with removal efficiencies between 37 and 50%. However, sulfate concentrations in the effluent were similar to those in the influent; removal rates were similar to those during period 2. Acidity remained in the same range (0.9–1.6 g L^{-1} as $CaCO_3$), while alkalinity increased significantly in columns #2 and #3, relative to period 2 (571 and 485 mg L^{-1} as $CaCO_3$, respectively). Alkalinity remained relatively constant for column #1 (496 mg L^{-1} as $CaCO_3$).

Period 4 (Days 230–291): 7 Day HRT and 4 g L^{-1} Fe

During period 4, significant increases were observed in iron concentrations (1.79–2.43 g L^{-1}), and its removal efficiency decreased to between 28 and 32%. At the same time, acidity increased to values similar to the first period (4.0 g L^{-1} $CaCO_3$), while sulfate concentrations also increased (9.8–10 g L^{-1}), corresponding to lower removal efficiencies (4–8%) relative to period 3 (7–11%). Other parameters, including pH (6.1), Eh (45–52 mV), and alkalinity (375–525 mg L^{-1} $CaCO_3$) showed only slight variations (Table 3).

Period 5 (Days 292–450): 5 Day HRT and 4 g L^{-1} Fe

During the final period, pH and Eh remained in the same range as period 4 (pH = 6.1 and Eh = 2357 mV). Iron removal efficiencies decreased (14–18%) and, as a result, alkalinity decreased as well (201–343 mg L^{-1} $CaCO_3$). Sulfate removal remained similar to period 4 (7–8%). Overall, most parameters were similar to those at the end of period 1 (similar operational conditions, after reaching the equilibrium). Therefore, the PBR columns #1, #2, and #3 maintained their efficiency and stability after 450 days of operation.

Evolution of Saturated Hydraulic Conductivity

The clogging of column PBRs can be assessed by k_{sat} values; a decrease in k_{sat} indicates reduced effective porosity due to pore filling due to the build-up of bacterial growth, physical deposition of fine particles, gas production, and biochemical precipitation of minerals (Anello et al. 2005; Bolis et al. 1992; Seki et al. 2006; Soleimani et al. 2009). In this study, k_{sat} decreased in column #3 (from 5.2×10^{-2} to 4.2×10^{-3} cm s^{-1}), whereas it remained stable in column #2 (2.1×10^{-3} cm s^{-1}). These findings are consistent with previous studies, including a decrease from 1×10^{-2} to 5×10^{-4} cm s^{-1} (URS 2003) and from 1×10^{-3} to 1×10^{-4} cm s^{-1} (Waybrant et al. 1998). Feeding the column PBRs with an upward flow may have reduced clogging (Bolis et al. 1992; URS 2003).

Evolution of Hydraulic Retention Time

The response of column #2 to a step-wise injection of NaCl showed that during the first 96 h, Cl^{-}concentrations remained relatively stable (201–280 mg L^{-1}), but progressively increased afterwards and stabilized at 2150 mg L^{-1} after 264 h (Fig. 2). According to the trend of Cl^{-} concentrations in the tracer test, which was not completely recovered, the system could be modeled as a succession of a plug flow reactor (with 96 h of HRT, i.e. latency period) and a continuous stirred reactor (with 34.7 h of HRT, i.e. increased Cl^{-} concentrations).

The total HRT of column #2 was estimated to be 5.4 days, corresponding to a porosity of 0.47, which is slightly higher than the initial value (0.41). The tracer test results did not

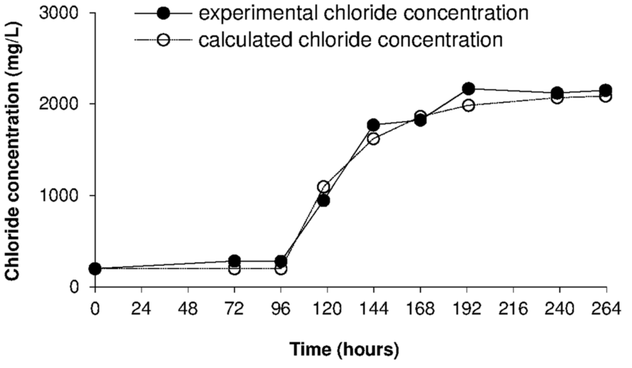

Fig. 2 Tracer test results

show any significant decrease in HRT with time or clogging. These findings were also confirmed by visual observations at the dismantling stage.

Characterization of the Spent Reactive Mixtures

Analyses of the solid samples of the spent reactive mixtures, collected after column dismantlement, showed an increase in the TOC/TKN ratio, corresponding to a loss of nitrogen relative to carbon, likely due to bacterial growth. These conditions could affect long-term bacterial viability and growth. In addition, DOC clearly decreased (14, 3, and 1% of the initial DOC concentrations for mixtures #1, #2, and #3, respectively).

Initial concentrations of total sulfur in samples from the top, middle, and bottom layers (0.6–1%) showed no significant differences between columns #1, #2, and #3. However, total sulfur increased (4, 3 and 2%, respectively). The SEP analyses showed that, regardless of the mixture, Al was mostly present in the residual fraction (86–93%; Table 4).

Only a small portion of the Al (1–9%) was bound to organic matter or to Fe-Mn oxyhydroxides. Visual MINTEQ modeling suggested that the precipitated Al hydroxides [boehmite, γ-AlO(OH); diaspore, α-AlO(OH); and gibbsite, α-Al$(OH)_3$] was probably the main Al sink. Most of the Al is probably originating from the reactive mixtures, which initially contained ≈ 1% Al.

The Cr fractionation was similar: 2–4% oxidizable or bound to organic matter, 23–55% reducible or bound to Fe–Mn oxides-hydroxides, and 40–69% in the residual fraction. Lead, however, was mostly retained in fraction 3 (up to 54%), 4 (3 to 40%), and 5 (up to 96%). The formation of reducible phases or Fe-Mn oxyhydroxide-bound phases (i.e. fraction 3) seemed to be the predominant mechanism for Zn retention (73–86%), followed by the formation of oxidizable or organic matter-bound phases (9–24%). The soluble and exchangeable fraction (fraction 1) of Ni was not negligible (6–12%), although its retention was mainly due to the formation of reducible phases or Fe–Mn oxyhydroxide-bound phases (37–64%), followed by the formation of oxidizable or organic matter-bound phases (16–38%). A similar trend was observed for Mn, for which Visual MINTEQ also suggested the formation of a carbonate phase, such as rhodochrosite [$Mn(CO_3)_2$]. The fractionation of Cd was notably different, with a high soluble or exchangeable fraction (0–50%). The other mechanism of Cd removal was the formation of reducible phases or Fe–Mn oxyhydroxide-bound phases (40–60%, depending on the mixture). Iron was mainly present in the reducible fraction or bound to the Fe–Mn oxyhydroxide fraction (51–67%), in the oxidizable or organic matter-bound fraction (14–17%), and in the residual fraction (8–26%). A small fraction of the iron was also bound to carbonates (6–10%), and as soluble or exchangeable species (1–4%). The precipitation of iron as carbonates, oxyhydroxides, and hydroxylsulfates [e.g. siderite, $FeCO_3$; ferrihydrite, $Fe_2O_3 \cdot 0.5(H_2O)$; goethite, α-FeO(OH); lepidocrocite, γ-FeO(OH); and schwertmannite, $Fe_8O_8(OH)_6(SO_4) \cdot nH_2O$] was also indicated by Visual MINTEQ. Total metal removal by mixtures #1, #2, and #3 amounted to 72, 47, and 61 mg g^{-1}, respectively, consistent with previously reported data (Neculita et al. 2008b).

With respect to initial metal concentrations (Al, Cd, Cr, Fe, Mn, Ni, Pb, and Zn) in reactive mixtures #1, #2, and #3 (which were, respectively, 17.0, 19.3, and 31.3 mg g^{-1}), SEP results showed double to triple final metal contents (at the end of testing), depending on the mixture. The SEP results and secondary electron images, with related repartition of the main chemical components of the reactive mixtures #1, #2, and #3 are presented in ESM 1 (Supplemental material accompanying the on-line version of this paper).

X-ray mapping is more appropriate for polished sample sections, whereas in the present study, unpolished materials were used. Results from the three mixtures showed a superposition of Fe, O, C, and Al. This observation confirms the precipitation of oxide or hydroxide phases of iron or aluminum on the surfaces of organic material (represented by carbon). The superposition of iron and sulfur suggested possible precipitation of iron sulfide in these two columns. However, sulfide mineral observations were hindered by the sample preparation technique. Because SEM analyses require dry samples, some biosulfides were probably oxidized. A similar observation could apply to the SEP approach.

Discussion

Performance of Passive Biochemical Reactors

After reaching steady-state, the PBRs' performance was mainly dependent on three design parameters: HRT, reactive

Table 4 Metal fractionation using a sequential extraction procedure in the reactive mixtures after dismantling of the columns

Mixture #	Fraction 1 (%)	Fraction 2	Fraction 3	Fraction 4	Fraction 5	Sum of fractions (mg g^{-1})
Al						
1	0	0	2	5	93	27.0
2	0	0	2	9	89	13.0
3	0	0	1	7	86	22.0
Cd						
1	50	11	40	0	0	7.7×10^{-4}
2	35	12	53	0	0	3.5×10^{-4}
3	0	40	60	0	0	1.1×10^{-4}
Cr						
1	0	0	4	55	40	8.0×10^{-3}
2	0	0	2	23	75	2.2×10^{-2}
3	0	0	4	27	69	2.4×10^{-2}
Fe						
1	1	10	67	14	8	44.0
2	3	6	61	17	14	32.0
3	4	6	51	15	26	38.0
Mn						
1	16	28	31	8	17	0.3
2	14	11	59	4	12	0.4
3	15	13	31	7	35	0.5
Ni						
1	6	9	64	21	0	0.1
2	12	6	37	38	7	4.7×10^{-2}
3	10	10	59	17	4	8.3×10^{-2}
Pb						
1	4	0	54	40	0	1.6×10^{-2}
2	0	0	0	3	96	1.4
3	2	0	44	13	44	2.3×10^{-2}
Zn						
1	1	3	76	21	0	0.5
2	1	2	73	24	0	0.2
3	1	4	86	9	0	0.2

Fraction 1: soluble and exchangeable metals; Fraction 2: carbonate-bound metals; Fraction 3: reducible or metals bound to Fe–Mn oxides; Fraction 4: oxidizable or metals bound to organic matter; Fraction 5: residual metals

mixture composition, and AMD quality (Neculita et al. 2007; USEPA 2014). Results showed that there were no significant differences among the three columns (#1, #2, and #3), which were used to evaluate three reactive mixtures, two HRTs, and two AMD qualities. The columns' performance, in terms of changes in pH, Eh, and alkalinity as well as iron and sulfate removal, were similar for given periods of time (Table 3). Column #1 yielded only slightly more favorable results, likely due to the higher organic substrate content relative to the other two columns (Genty et al. 2017), which contained 50% sand or calcitic sand. A longer HRT promoted increased alkalinity generation, regardless of the AMD quality. Changing the HRT from 7 to 5 days (periods 4–5) decreased alkalinity from between 525 and 375 to between 343 and 201 mg L^{-1}, as $CaCO_3$, depending on the reactive mixture. Iron removal was similarly affected, with decreases from 32 to 22% to 18–14%. In contrast, increasing the HRT from 5 to 7 days (periods 2–3) decreased iron concentrations from 955–980 mg L^{-1} to 615–732 mg L^{-1}.

The overall performance of PBRs treating iron-rich AMD is greatly influenced by total iron concentration (Genty et al. 2017; Neculita et al. 2008a). With a 5 day HRT, less iron removal was found for AMD with 1 g L^{-1} Fe (14–18%, period 2), than AMD with 4 g L^{-1} Fe (27–33%, period 5). With a 7 day HRT, the opposite result was found; i.e. iron removal decreased from 37 to 50% (period 3, 1 g L^{-1} Fe) to 22–32% (period 4, 4 g L^{-1} Fe). A shorter HRT did not provide the appropriate conditions for precipitation of iron hydroxides, and, given the high degree of contamination, the SRB were probably not efficient enough in producing soluble sulfides.

Special emphasis in the present study was given to iron treatment; however, the performance of column-type PBRs was also evaluated for other metals contained in the synthetic AMD sample. Removal of Al, Cd, Cr, Ni, and Zn were always over 90%; Pb removal was between 52 and 80%, and Mn removal was between 1 and 28%. No significant differences in metal removal were observed among the three reactive mixtures. Therefore, the addition of 50–60% of sandy material neither improved nor reduced metal retention. The removal of Mn was marginal, which is consistent with findings from similar studies (Neculita et al. 2008a; Song et al. 2012a). The causes of poor Mn removal efficiency include: the inhibition of precipitation due to Fe:Mn ratios above 2:3; reductive dissolution of Mn oxides in the presence of agents (such as Fe^{2+}, sulfides, and organic acids); and the preferential complexation of other metals with sulfides (Song et al. 2012a).

Sulfate removal remained below 24% for all treatment periods (after 55 days), regardless of the column (Table 3), and was similar for both AMD qualities and the two tested HRTs. The DOC/SO_4 ratio was very low, which indicates a severe lack of the DOC required for bacterial growth and could explain the low sulfate removal (Neculita and Zagury 2008). Indeed, the DOC/SO_4 ratio in the mixtures decreased from initial values of 0.0133 (#1), 0.0156 (#2), and 0.0567 (#3) to 0.004 (#1), and to 0.0009 (#2 and #3), at the end of testing.

Additional organic carbon in the reactive mixture of PBRs treating iron-rich AMD, with relatively constant release of DOC over time, is warranted. Previously reported findings showed more rapid exhaustion of DOC at pH 3 relative to pH 6 (Song et al. 2012b). For a sulfate concentration of 9 g L^{-1}, ≈ 3.6 g L^{-1} DOC would be required to give an optimal DOC/sulfate ratio for sulfate reduction; i.e. 0.4 (Neculita and Zagury 2008).

Conclusion

We evaluated the effectiveness of five passive biochemical reactors and temporal changes in their hydraulic parameters (i.e. k_{sat} and HRT) during the treatment of ferriferous AMD over a 450 day period. Two synthetic, iron-rich AMD qualities (1 and 4 g L^{-1}), two HRTs (5 and 7 days), and three reactive mixture compositions (which were previously proven to be effective in batch testing) were tested. Column PBRs increased the pH from 3.5 to 6 and efficiently removed Al, Cd, Cr, Ni, Pb, and Zn (> 90%). However, Fe concentrations remained high (3.2 to 3.4 g L^{-1}), especially after day 230; this resulted in high acidity and pH decreases in the treated effluents within a few hours of exposure to air. Metal removal efficiency was only slightly affected by the HRT, which, only increased alkalinity generation when HRT was increased from 5 to 7 days. Differences in the efficiencies of the three tested mixtures were not significant. Adding 50% of a structural agent did not affect metal removal. Measurements of k_{sat} for mixtures with (50% w/w) and without sand or calcitic sand (#2 and #3, respectively) showed no improvement of hydraulic properties. The k_{sat} remained relatively stable (2.1×10^3 cm s^{-1} for column #2 and 9.9×10^3 cm s^{-1} for column #3) for more than a year. Tracer tests carried out at the end of the experiment showed no significant changes in mixture porosity, and thus confirmed that clogging was not the principal cause of the limited efficiency. Although sorption could have played an important role at the start-up of the PBRs, Fe was mainly removed by precipitation (as oxyhydroxides in aerobic conditions and biosulfides in anaerobic conditions). However, sulfate reduction was not the predominant mechanism of Fe removal. Given the marginal effectiveness of the PBRs for ferriferous AMD treatment, a multi-step system should be considered, including an iron pre-treatment step.

Acknowledgements This research was funded by the Canada Research Chair on Restoration of Abandoned Mine Sites and the Natural Sciences and Engineering Research Council of Canada (NSERC) through the NSERC Polytechnique-UQAT Industrial Chair on the Environment and Mine Waste Management. The authors gratefully acknowledge the industrial and governmental partners of the industrial Chair for funding this study.

References

AFNOR (Association Française de Normalisation) (1986) Testing water—determination of sulphate ions—nephelometric method. AFNOR—NF T90–040, St Denis, France

Anello G, Lamarche P, Héroux JA (2005) Reduction of hydraulic conductivity changes in an in-ground bioreactor. J Environ Eng Sci 4:195–207

APHA (American Public Health Assoc) (2005) Standard methods for the examination of water and wastewater, 20th edn. In: Clesceri LS, Greenberg AE, Eaton AD (eds) American Public Health Assoc, American Water Works Assoc, Water Environment Federation, APHA-AWWA-WEF, Washington, DC

ASTM (American Society for Testing Materials) (1995) Standard test method for permeability of granular soils. ASTM International, West Conshohocken, pp D 2434–2468

ASTM (American Society for Testing Materials) (2009) Standard methods for sulphate reducing bacteria in water and waterformed deposits. ASTM International, West Conshohocken, pp D 4412–4484

Ayora C, Caraballo MA, Macias F, Rötting TS, Carrera J, Nieto JM (2013) Acid mine drainage in the Iberian pyrite belt: lessons learned from recent passive remediation experiences. Environ Sci Pollut R 20:7837–7853

Baldwin SA, Khoshnoodi M, Rezadehbashi M, Taupp M, Hallam S, Mattes A, Sanei H (2015) The microbial community of a passive biochemical reactor treating arsenic, zinc, and sulfate-rich seepage. Biotechnol Bioeng 3(27):1–13

Bolis JL, Wildeman TR, Dawson HE (1992) Hydraulic conductivity of substrates used for passive acid mine drainage treatment. In: Proc national meeting of american soc for surface mining and reclamation, Duluth, pp 79–89

Butler BA, Smith ME, Reisman DJ, Lazorchak JM (2011) Metal removal efficiency and ecotoxicological assessment of field-scale passive treatment biochemical reactors. Environ Toxicol Chem 30:385–392

Champagne P, Van Geel P, Parker W (2005) A bench-scale assessment of a combined passive system to reduce concentrations of metals and sulphate in acid mine drainage. Mine Water Environ 24:124–133

Chang IS, Shin PK, Kim BH (2000) Biological treatment of acid mine drainage under sulfate-reducing conditions with solid waste materials as substrate. Water Res 34:1269–1277

Fogler HS (2006) Element of chemical reaction engineering, 4th edn. International series in the physical and chemical engineering sciences. Prentice Hall International Inc, Upper Saddle River, NJ, USA, p 1120

Genty T, Bussière B, Neculita CM, Benzaazoua M, Zagury GJ (2011) Passive treatment of acid mine drainage: repeatability for sulphate reducing passive bioreactor column efficiency testing. In: Proc IMWA Congress, Aachen, pp 313–318

Genty T, Bussière B, Potvin R, Benzaazoua M, Zagury GJ (2012a) Dissolution of different limestone in highly contaminated acid mine drainage: application to anoxic limestone drains. Environ Earth Sci 66:2387–2401

Genty T, Bussière B, Benzaazoua M, Zagury JG (2012b) Capacity of wood ashes filters to remove iron from acid mine drainage: assessment of metal retention mechanisms. Mine Water Environ 31:273–286

Genty T, Bussière B, Paradis M, Neculita CM (2016) Passive biochemical treatment of ferriferous mine drainage: Lorraine mine site, Northern Quebec, Canada. In: Proc international mine water assoc (IMWA), Conf, pp 790–795

Genty T, Bussière B, Benzaazoua M, Neculita CM, Zagury GJ (2017) Efficiency of iron removal during the treatment of highly contaminated acid mine drainage in biochemical reactors. Water Sci Technol 76(7):1833–1843

Lewis AE (2010) Review on metal sulphide precipitation. Hydrometallurgy 104:222–234

Mendelhall W, Beaver RJ (1994) Introduction to probability and statistics, 9th edn. Duxbury Press, Belmont

Moncur MC, Ptacek CJ, Blowes DW, Jambor JL (2005) Release, transport and attenuation of metals from an old tailings impoundment. Appl Geochem 20:639–659

Neculita CM, Zagury GJ (2008) Biological treatment of highly contaminated acid mine drainage in batch reactors: long-term treatment and reactive mixture characterization. J Hazard Mater 157:358–366

Neculita CM, Zagury GJ, Bussiere B (2007) Passive treatment of acid mine drainage in bioreactors using sulfate-reducing bacteria: critical review and research needs. J Environ Qual 36:1–16

Neculita CM, Zagury GJ, Bussiere B (2008a) Effectiveness of sulphate-reducing passive bioreactors for treating highly contaminated acid mine drainage: I. Effect of hydraulic retention time. Appl Geochem 23:3442–3451

Neculita CM, Zagury GJ, Bussiere B (2008b) Effectiveness of sulphate-reducing passive bioreactors for treating highly contaminated acid mine drainage: II. Metal removal mechanisms and potential mobility. Appl Geochem 23:3545–3560

Neculita CM, Vigneault B, Zagury GJ (2008c) Toxicity and metal speciation in acid mine drainage treated by passive bioreactors. Environ Toxicol Chem 27:1659–1667

Postgate JR (1984) The sulfate-reducing bacteria, 2nd edn. Cambridge Univ Press, Cambridge

Rakotonimaro TV, Neculita CM, Bussière B, Zagury GJ (2016) Pretreatment of iron-rich acid mine drainage using various dispersed alkaline substrates. Appl Geochem 73:12–23

Rakotonimaro TV, Neculita CM, Bussière B, Zagury GJ (2017) Comparative column testing of three reactive mixtures for the biochemical treatment of iron rich acid mine drainage. Miner Eng 11:79–89

Rötting T, Caraballo M, Serrano J, Ayora C (2008) Field application of calcite dispersed Alkaline Substrate (calcite-DAS) for passive treatment of acid mine drainage with high Al and metal concentrations. Appl Geochem 23:1660–1674

Seki K, Thullner M, Hanada J, Miyazaki T (2006) Moderate bioclogging leading to preferential flow paths in biobarriers. Ground Water Monit R 26:68–76

Seo J, Kwon D, Yoon TH, Jung J (2010) Potential risks of the natural nanoparticles from the acid mine drainage and a novel approach for their toxicity assessment. Toxicol Environ Health Sci 2:215–220

Skousen J, Zipper CE, Rose A, Ziemkiewicz PF, Nairn R, McDonald LM, Kleinmann RL (2017) Review of passive systems for acid mine drainage treatment. Mine Water Environ 36:133–153

Soleimani S, Van Geel P, Isgor B, Mostafa M (2009) Modeling of biological clogging in unsaturated porous media. J Contam Hydrol 106:39–50

Song H, Yim GJ, Ji SW, Neculita CM, Hwang TW (2012a) Pilot-scale passive bioreactors for treatment of natural acid mine drainage: efficiency of mushroom compost vs. mixed substrates for metal removal. J Environ Manage 111:150–158

Song H, Yim GJ, Ji SW, Nam IH, Neculita CM, Lee GY (2012b) Performance of mixed organic substrates during the treatment of acidic and moderate mine drainage in column bioreactors. J Environ Eng ASCE 138:1077–1084

URS (United Registrar of Systems) (2003) Passive and semi-active treatment of acid rock drainage from metal mines-state of the practice. Prepared for US Army Corps of Engineers, Concord

USEPA (United States Environmental Protection Agency) (2014) Reference guide to treatment technologies for mining-influenced water. EPA 542-R-14–001. https://www.epa.gov/remedytech/reference-guide-treatment-technologies-mining-influenced-water. Accessed 29 Oct 2017

Waybrant KR, Blowes DW, Ptacek CJ (1998) Selection of reactive mixtures for use in permeable reactive walls for treatment of acid mine drainage. Environ Sci Technol 32:1972–1979

Younger PL, Banwart SA, Hedin RS (2002) Mine water: Hydrogeology, pollution, remediation. In: Alloway BJ, Trevors JT (eds) Kluwer Academic Publ, Dordrecht, The Netherlands, p 442

Zagury GJ, Colombano SM, Narasiah KS, Ballivy G (1997) Stabilisation de résidus acides miniers par des résidus alcalins d'usines de pâtes et papier. Environ Technol 18:959–973

Zagury GJ, Kulnieks V, Neculita CM (2006) Characterization and reactivity assessment of organic substrates for sulphate-reducing bacteria in acid mine drainage treatment. Chemosphere 64:944–954